Micromechanical properties and structural characterization of modern inarticulated brachiopod shells

C. Merkel,[1] E. Griesshaber,[2] K. Kelm,[3] R. Neuser,[4] G. Jordan,[1] A. Logan,[5] W. Mader,[3] and W. W. Schmahl[1]

[1] We investigated micromechanical properties and ultrastructure of the shells of the modern brachiopod species *Lingula anatina*, *Discinisca laevis*, and *Discradisca stella* with scanning electron microscopy (SEM, EDX), transmission electron microscopy (TEM) and Vickers microhardness indentation analyses. The shells are composed of two distinct layers, an outer primary layer and an inner secondary layer. Except for the primary layer in *Lingula anatina*, which is composed entirely of organic matter, all other shell layers are laminated organic/inorganic composites. The organic matter is built of chitin fibers, which provide the matrix for the incorporation of calcium phosphate. Amorphous calcium phosphate in the outer, primary layer and crystalline apatite is deposited into the inner, secondary layer of the shell. Apatite crystallite sizes in the umbonal region of the shell are about 50×50 nm, while within the valves crystallite sizes are significantly smaller, averaging 10×25 nm. There is great variation in hardness values between shell layers and between the investigated brachiopod species. The microhardness of the investigated shells is significantly lower than that of inorganic hydroxyapatite. This is caused by the predominantly organic material component that in these shells is either developed as purely organic layers or as an organic fibrous matrix reinforced by crystallites. Our results show that this particular fiber composite material is very efficient for the protection and the support of the soft animal tissue. It lowers the probability of crack formation and effectively impedes crack propagation perpendicular to the shell by crack-deviation mechanisms. The high degree of mechanical stability and toughness is achieved by two design features. First, there is the fiber composite material which overcomes some detrimental and enhances some advantageous properties of the single constituents, that is the softness and flexibility of chitin and the hardness and brittleness of apatite. Second, there is a hierarchical structuring from the nanometer to a micrometer level. We could identify at least seven levels of hierarchy within the shells.

1. Introduction

[2] Fundamental interest in biogenic materials providing biomechanical support or protective structures arises from the fact that they share many design features with advanced engineering materials. Thus they may serve as prototypes for new developments in the design of structural or functional materials (see, e.g., *Wegst and Ashby* [2004] or *Oyen et al.* [2006] for recent overviews of mechanical properties of biomaterials). Biogenic hard tissues such as shells and skeletons are hybrid (i.e., organic/inorganic) composites, since they contain a certain amount of organic material which surrounds a mineral phase [*Aizenberg et al.*, 2005; *Mayer*, 2005; *Gilbert et al.*, 2005]. Even though the organic material may represent a very small volume fraction ($\sim$1%) it exerts a fundamental control on the nucleation and growth of the entire hybrid composite system. It is the key factor for the hierarchical organization of the biomaterial [e.g., *Currey*, 2005; *Rousseau et al.*, 2005] as well as the controlling agent for the development of its distinct multifunctional properties [*Mayer and Sarikaya*, 2002; *Cölfen and Mann*, 2003; *Sarikaya et al.*, 2004]. A strong influence on the crystallographic orientation of the biomineral constituents [*Iijima and Moriwaki*, 1990; *Schmahl*

[1]Section of Applied Crystallography and Materials Science, Department of Earth and Environmental Sciences, Ludwig-Maximilians University Munich, Munich, Germany.

[2]Section of Palaeontology, Department of Earth and Environmental Sciences, Ludwig-Maximilians University Munich, Munich, Germany.

[3]Institut für Anorganische Chemie, Universität Bonn, Bonn, Germany.

[4]Institut für Geologie, Mineralogie und Geophysik, Ruhr-Universität Bochum, Bochum, Germany.

[5]Department of Physical Sciences, University of New Brunswick, Saint John, New Brunswick, Canada.

et al., 2004] is provided by the organic matrix. Functional properties such as stiffness and hardness of the biomaterial can be altered by changing the ratio of the organic to inorganic components or the structural organization on any length scale. Notably crack propagation within the shells [*Griesshaber et al.*, 2007] and bones [*Currey*, 2002] is greatly reduced by the presence of organic fibers, membranes and organic layers [*Kamat et al.*, 2000; *Okumura and de Gennes*, 2001; *Ji and Gao*, 2004].

[3] While the relationship between microstructure and micromechanical properties, such as hardness, crack formation and crack deviation, is well studied for biological aragonite [*Laraia and Heuer*, 1990; *Kamat et al.*, 2000; *Aizenberg et al.*, 2005], biological calcite [*Griesshaber et al.*, 2007] and biological silica [*Sarikaya et al.*, 2001; *Sundar et al.*, 2003], this has been done to a much lesser extent for marine biological phosphate. Mechanical properties of inarticulated (phosphatic) brachiopod shells are unknown. In order to gain a more complete understanding of the microstructure and micromechanical properties of shells of marine organisms we have extended our previous studies on calcitic brachiopod shells [e.g., *Griesshaber et al.*, 2005, 2007] to phosphatic forms. For this purpose SEM and TEM imaging of *Lingula anatina*, *Discinisca laevis* and *Discradisca stella* has been combined with Vickers microhardness analysis. Brachiopods in general (phosphatic as well as calcitic genera) are ideal for a wide range of studies, such as evolutionary systematics [e.g., *Williams et al.*, 1994, 1997, 1998a] and variations in oceanographic conditions [e.g., *Veizer et al.*, 1999; *Bruckschen et al.*, 1999; *Brand et al.*, 2003; *Parkinson et al.*, 2005], as well as for the study of biomineralization processes and properties of biomaterials [e.g., *Schmahl et al.*, 2004; *Griesshaber et al.*, 2007]. Brachiopods have existed since the late Proterozoic, they occur in a wide range of marine environments and they are still extant in several marine habitats, so they are well suited to such studies.

[4] The aim of this study is threefold: (1) to assess the internal architecture of phosphatic brachiopod shells with an enhanced resolution, (2) to explain micromechanical variations within phosphatic brachiopod shells and relate them to microstructural observations, and (3) to compare the results with those obtained on calcitic forms and other phosphatic biomaterials.

2.   Sample Preparation and Analytical Techniques

[5] We investigated specimens of the modern phosphatic brachiopod species *Lingula anatina* (taken from shallow coastal waters in Japan), *Discinisca laevis* (taken from 0.5 m water depth in Namibia) and *Discradisca stella* (taken from 10 m water depth in Bali, Indonesia). For all analyses, SEM, EDX, Vickers microhardness and TEM cross and longitudinal sections were cut relative to the median plane of the shell. The obtained wafers were then prepared on both sides as highly polished, uncovered 150 micrometer thick sections coated either with vapor deposited graphite, or, in the case of broken shell fragments, with sputtered gold particles. For TEM studies, oriented shell fragments were cut out from a 500 micrometer thin section with a microtome. Subsequently, these microtome sections were

thinned down to a thickness of about 30 micrometers through a combination of grinding and dimple grinding. The final Ar^+ ion-beam thinning created holes with wedge-shaped electron-transparent edges.

[6] SEM images and EDX analyses were performed on a LEO Gemini 1530 SEM, equipped with an HKL Technology Channel 5 EBSD system and an SiLi-based EDX detector (OXFORD ISIS) for chemical characterization of the sample. TEM observations were carried out on a Phillips CM30T electron microscope equipped with an EDX system constructed by Noran and an HPGe detector. Microhardness investigations were carried out with an Aquinto analyzer system, where the used microindenter complied to the DIN 50133 standard. Indentations were applied at room temperature on air-dried samples. Two distinct forces 0,49 N and 0.049 N were applied for the indentation. In both cases the force was held during the indentation on the sample for 10 seconds. A force of 0.49 N corresponds to the Vickers hardness unit HV 0.05/10, whereas the force of 0.049 N corresponds to the HV 0.005/10 unit. The reproducibility of Vickers microhardness measurements on a homogeneous glass or metal standard is 5 HV.

[7] In order to visualize distinct shell structures with SEM the specimens were treated chemically and enzymatically. For demineralization experiments we used pH-neutral 0.2 M ethylenediaminetetraacetic acid. The organic shell components were digested by proteinase-K (0.3 mg/mL) which was admixed to a pH-neutral buffer solution of disodium-hydrogenphosphate (100 mMol/L). To degrade both organic and inorganic compounds we used a bleach solution of 3.5% sodium hypochlorite of pH 10. These solutions were applied to the samples for 24 hours. Subsequently, they were washed twice for 10 minutes with distilled water and dried for 24 hours at 60°C.

3.   Results

3.1.   General Shell Structure of *Lingula anatina*, *Discinisca laevis*, and *Discradisca stella*

[8] A strongly layered shell structure is the overall architectural feature of the shell of the investigated modern brachiopod species of the species *Lingula anatina, Discinisca laevis* and *Discradisca stella*. The layers are composed of arrays of chitin fibers with the degree of mineralization varying greatly from layer to layer. The mineralization consists of either nanoparticles of amorphous calcium phosphate or of crystalline apatite, which are attached to chitin fibers.

[9] An organic outer membrane, the periostracum, coats the shells of all brachiopods. Its width and habit varies for the different investigated brachiopod taxa. The periostracum of *Lingula anatina* is about 2.5 micrometers thick and can be subdivided into two layers. In *Discinisca laevis* the periostracum is rippled and its thickness varies greatly owing to a random incorporation of minute external particles. At its thickest parts it reaches about 20 micrometers. Similarly, periostracum thickness of *Discradisca stella* is uneven and ranges between 0 and 4 micrometers. The shell of all studied species can be subdivided into two sublayers, an outer primary (PL), and an inner secondary (SL) shell layer. In *Lingula anatina* the primary layer is composed entirely of organic matter, while in *Discinisca laevis* and
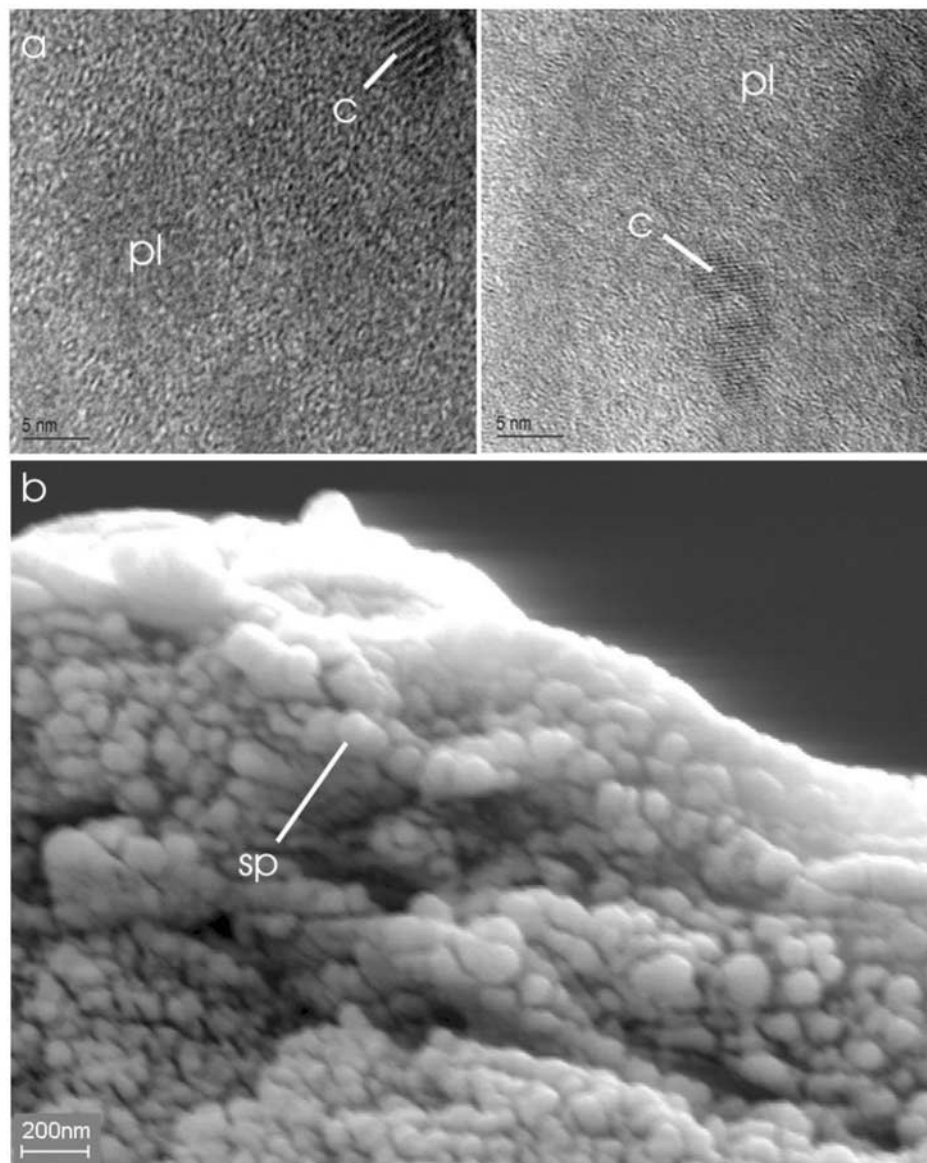
Figure 1. Electron microscopic images of the primary layer (pl) of *Discradisca stella*. (a) TEM images showing a spotty contrast characteristic of amorphous material with occasional occurrences of apatite crystals (location c) with a few nanometers in size. (b) SEM image showing spheroidal, amorphous apatite particles (sp) with sizes of 50–100 nm arranged around an organic (chitin) axial filament. These organic/inorganic composites form long twisted chains that are packed into arrays. A series of these arrays builds the primary layer of the shell.

Discradisca stella this layer is a composite of an organic matrix and amorphous Ca-phosphate or occasionally crystalline apatite. The thickness of the primary layer varies in the investigated specimens between 30 and 40 micrometers.

[10] TEM and SEM images (Figures 1a and 1b) of the primary layer of *Discradisca stella* show that this shell layer is composed of chitin fibers into which calcium phosphate particles are embedded. Our TEM investigations reveal predominantly amorphous calcium phosphate (ACP), with only occasional occurrences of minute apatite crystals (Figure 1a). This observation is in contrast to previous work, that has claimed that the primary layer of calcium-phosphatic inarticulate brachiopods can be regarded as an intercalation of beta-chitin fibers and apatite-like minerals,

such as francolite or carbonate-substituted hydroxyapatite [*Williams et al.*, 1998a; *Williams and Cusack*, 1999; *Lévêque et al.*, 2004]. As presented in Figure 1b, particle sizes of Ca-phosphate in the studied species are quite homogeneous and are around 50 nm. These particles occur with a spheroidal morphology, they are aligned onto twisted chains (Figure 1b) [*Iwata*, 1981; *Williams et al.*, 1994] and build a layered compound structure of chitin and amorphous calcium phosphate (Figure 2).

[11] The inner, secondary shell layer of the investigated species consists of a fiber composite structure, where inorganic particles are embedded in an organic matrix. Chitin fibers and an interconnecting proteinaceous coat
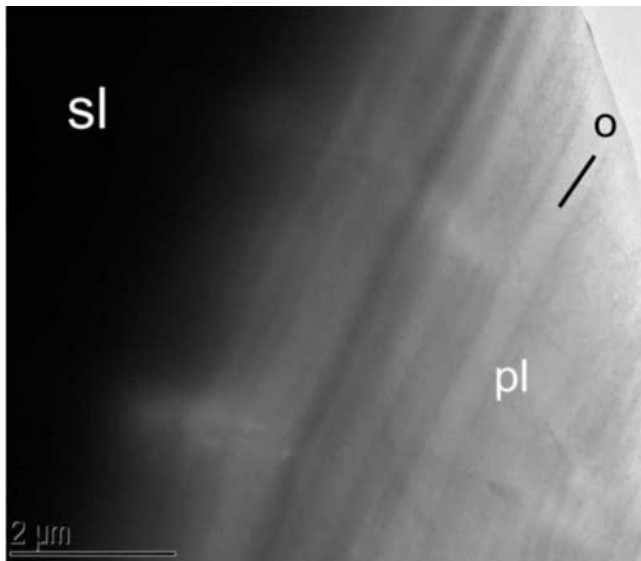
Figure 2. TEM picture of the transition between the primary (pl) and the secondary layer (sl) in the shell of *Discradisca stella*. Black and white stripes within the primary layer indicate a laminated organic/inorganic composite structure (o) with a thickness of the lamina in the 100 nm range.

[*Williams et al.*, 1994] serve as substrates for the calcium phosphate phase, which, in contrast to the outer, primary shell layer is predominantly crystalline (Figure 3a). The size of crystallites varies in different portions of the shell. In *Discradisca stella*, for example, crystals at the umbo (the oldest part of the shell) are rounded and are about 50×50 nm in size (Figure 3b), whereas crystals closer to the marginal fold are slightly elongated and have sizes around 10×25 nm (Figure 3c). Crystals within the umbonal region in *Discradisca stella* occasionally exhibit an hexagonal shape and thus have, although of biogenic origin, the morphology of inorganic apatite. The thickness of the secondary layer of the investigated specimens is several hundred micrometers, $600-800$ micrometers in *Lingula anatina*, 400 to 600 micrometers in *Discradisca stella* and 200 to 400 micrometers in *Discinisca laevis*.

[12] Rhythmic organic/inorganic laminates characterize the secondary layer of *Lingula anatina*. The basic unit in *Lingula anatina* (Figure 4) begins with a thin organic membrane, which is followed by a highly mineralized compact layer, followed by a considerably less mineralized transitional layer. This basic unit end with an organic layer again, which is significantly thicker than the starting organic membrane. As observable in Figure 4 this sequence is repeated within the shell several times. However, although the basic unit described above is always present, in the anterior shell region organic layers are predominant, while in the posterior shell region the highly mineralized compact layers are prevail.

[13] The internal structure of the secondary layer of *Discradisca stella* resembles closely that of *Discinisca laevis* [see *Williams et al.*, 1998b] and can also be described by an alternating sequence of organic and inorganic layers. In contrast to *Discinisca laevis*, *Discradisca stella* shows an inhomogeneous fracture behavior. In the outer part of the secondary shell ($\sim$300 micrometers, directly beneath the primary layer) the polished surface is corrugated as can be seen from Figure 10 in section 3.2 and in SEM images of fracture surfaces (not shown). In the inner part, the polished surface as well as the fracture surface is planar. We refer to this fracture behavior as a brittle or a cleaving fracture. Baculate structures (Figures 5a–5d) are the most conspicuous architectural features of the secondary shell layer of *Discradisca stella*. These structures are strings (Figures 6a and 6b) of organic fibers onto which apatite crystallites are attached. They bridge two compact sublayers. The compact layers can be described as compact and parallel arrays of baculi (Figure 5). The location of the baculate structures is shown in Figure 8b in section 3.2.

Figure 3. TEM images of the secondary layer of *Discradisca stella* at different magnifications. (a) As obvious from the lattice planes, the secondary shell layer contains significantly more crystalline apatite (cr) than the primary layer (Figure 1a). (b) Image showing three nanometer-sized apatite crystallites from the umbo region of the secondary layer of *Discradisca stella*. The crystallites are separated from each other by a small amount of organic (adhesive) material (m). (c) Image showing an elongated crystal from the secondary layer of the shell of *Discradisca stella*. These elongated crystallites are typical in the region located close to the marginal fold of the shell.
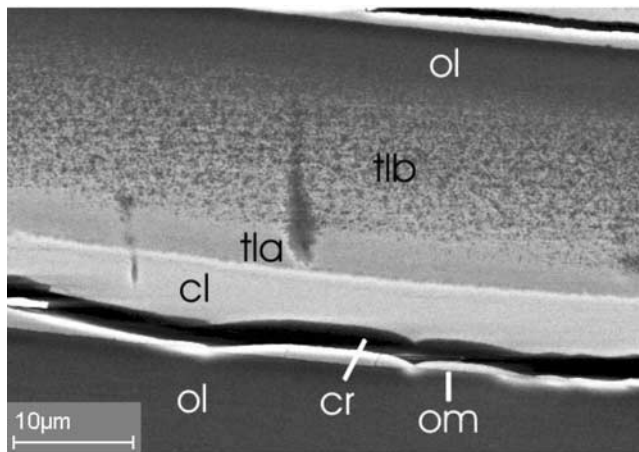
Figure 4. SEM image indicating the sequence of a rhythmic unit within the secondary shell layer of *Lingula anatina*. A rhythmic unit starts with an organic membrane (om), which is followed by a strongly mineralized compact layer (cl), a significantly less mineralized transitional layer (tla and tlb) and ends with a thick entirely organic layer (ol). Cracks (cr) typically appear in the compact layer.

3.2. Vickers Microhardness Distribution Patterns

[14] Vickers microhardness analyses for the three brachiopods are given in Figures 7, 8 and 9. It should be noted that the indentations were performed with two different forces: 0.49 N and 0.049 N. A force of 0.49 N was used for the measurement of the overall hardness distribution pattern (Figures 7a, 8a, 8b, 9a). The obtained values refer to the inner (secondary) layer, since the indents are too large for the thickness of the thin primary layer. For an investigation of all sublayers of the primary and the secondary layer indentations with the small force were carried out. These are shown in Figures 7b–7g, 8c and 9b.

[15] In comparison to the microhardness measured on inorganic hydroxyapatite (250 < Vickers microhardness < 300 HV0.05/10), the hardness of the shells of *Lingula anatina*, *Discinisca laevis* and *Discradisca stella* is significantly lower. This is in marked contrast to the hardness behavior of calcitic brachiopods, where in comparison to inorganic calcite both, lower but also much higher microhardness values have been obtained [*Griesshaber et al.*, 2005, 2007].

[16] Significant differences in microhardness occur between the three investigated brachiopod genera. The microhardness of *Lingula anatina* varies between 23 and 192 HV 0.05/10, that of *Discinisca laevis* between 34 and 90 HV 0.05/10 and that of *Discradisca stella* between 63 and 163 HV 0.05/10, respectively. While microhardness values between 23 and 25 HV 0.05/10 are representative for the purely organic layers of *Lingula anatina*, the highest microhardness values of 192 HV 0.05/10 are present in the compact, highly mineralized shell regions of the body platform. *Discinisca laevis* shows the lowest microhardness values of all three investigated brachiopod genera. This can be explained by a higher fraction of organic matter within the shell of this brachiopod, but it can also be attributed to the presence of micropores, which are oriented parallel to the shell outer surface and perpendicular to the shell

growth direction. The microhardness values in *Discradisca stella* along the innermost shell region, next to the soft organic parts of the animal, scatter around 110 HV 0.05/10, the highest hardness (120–160 HV 0.05/10) occurs within the central portion of the shell, while the lowest micro-
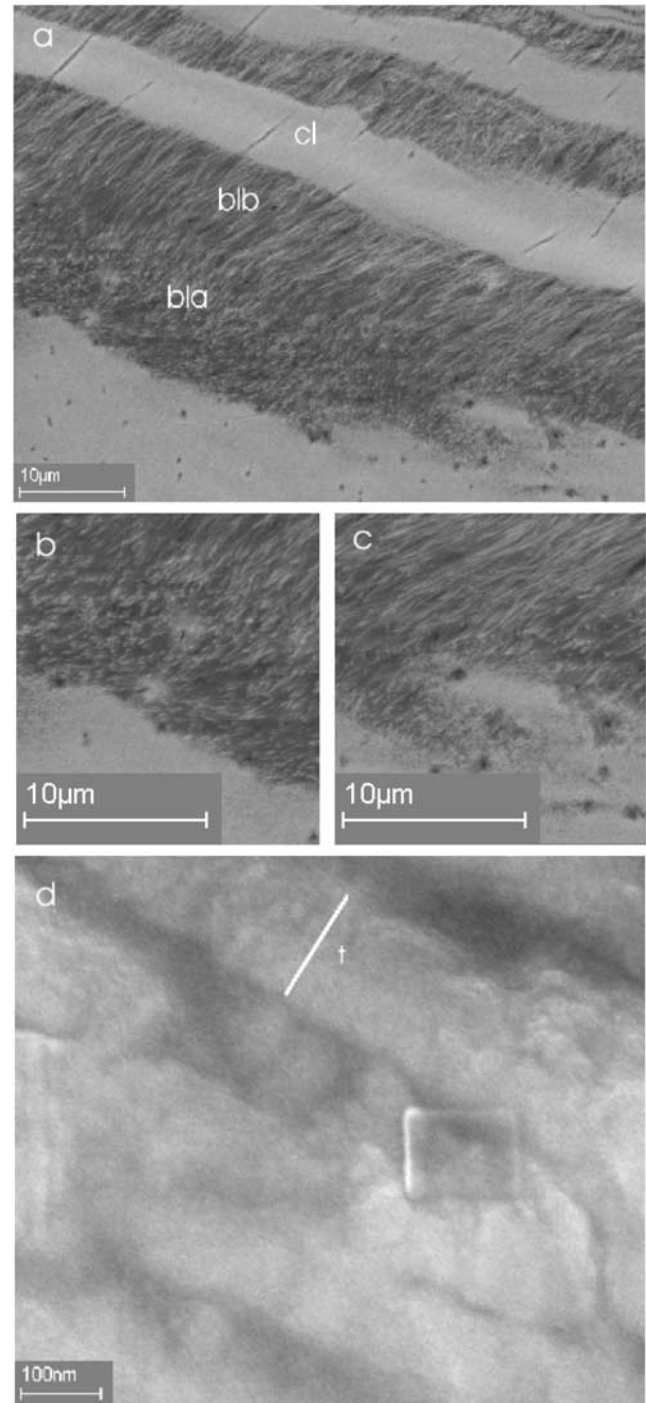

Figure 5. TEM image of the secondary shell layer of *Discradisca stella.* (a) Baculate structures (bla and blb) are shown that bridge two highly mineralized compact laminae within the shell. (b, c) Magnifications from Figure 5a. (d) TEM image showing the ~120-nm-wide individual mineralized fibers (baculi).
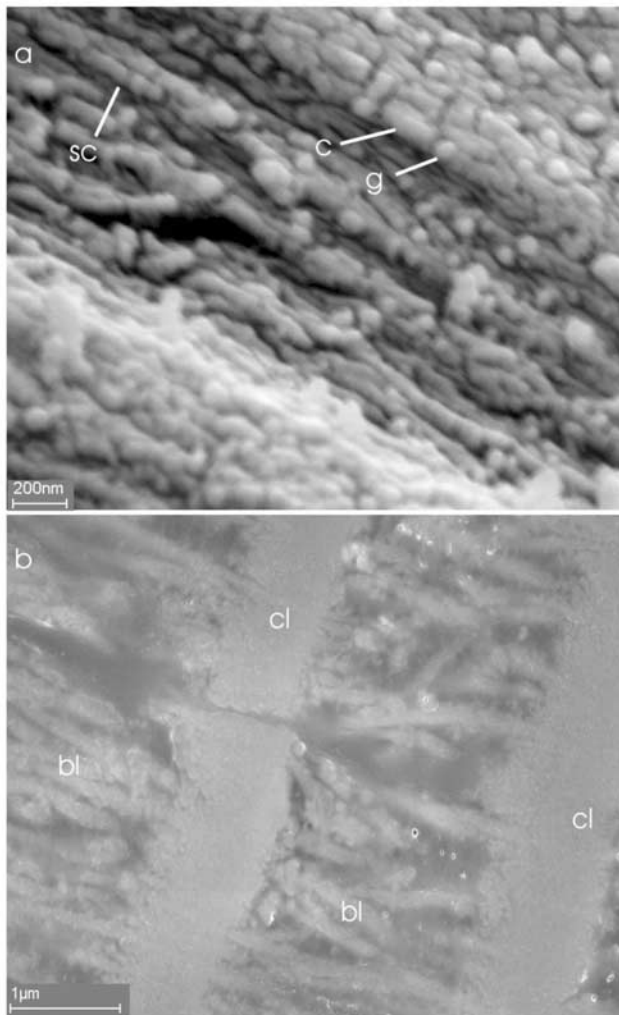
Figure 6. SEM images of mineralized fibers in the secondary layer of *Discradisca stella*. (a) stacked chains (sc) of highly mineralized organic fibers form the compact layer of *Discradisca stella*. Apatite crystals occur either in granuline (g) or cylindric (c) arrangements. (b) The thickness (t) of mineralized organic fibers scatters between 80 and 160 nm.

hardness (85HV 0.05/10) has been measured along the outermost shell segments.

[17] Figure 7b–7e show indentations along a profile ranging from the outer to the innermost layer of the shell of *Lingula anatina*. The values for microhardness indents which have been placed in the more strongly mineralized sections of the shell are underlined, while the other values correspond to indentations which were placed in the organic-rich segments. Vickers indents in phosphatic shells show a regular pyramidal appearance in contrast to those in calcitic shells, where fracturing and delamination is observed around the indents. The ductility of the phosphatic shells can be attributed to the higher amount of organic material, the fibrous nature of the organics and the nanoscopic particle size of the inorganic component. As observable in Figures 7b–7e the more strongly mineralized lamellae of the shell are harder and have hardness values that scatter

between 80 and 260 HV 0.05/10. The shell becomes softer along its inner side. A mineralized and organic-rich interlayering is observable, where toward the innermost layer of the shell the organic-rich sublayer becomes predominant (Figures 7f and 7g). The innermost layer is highly organic-dominated and has a Vickers hardness of 26 to 27 HV 0.05/10. In general, we observe for both types of indents, those placed into the mineralized and those placed into the organic-rich lamellae, a decrease in hardness values from the outer to the innermost part of the shell (see Figures 7d and 7e). This can clearly be attributed to an increased fraction of organic material. In *Lingula anatina* we observe an interlayering between mineralized and organic-rich layers on two scale levels (Figures 7f and 7g). One scale level is given in Figure 7f, where mineralized and organic-rich sublayers alternate with a period in the range of 30 micrometer. Figure 7g shows the interlayering on a higher scale level. The organic-rich sublayers can themselves be regarded as interlayerings between organic and mineralized lamellae.

[18] Figures 8c and 9b show the detailed hardness distribution patterns in the shell of *Discradisca stella* and *Discinisca laevis*. These brachiopod species do not show the simple outer hard-inner soft distribution pattern of hardness of the secondary layer of *Lingula anatina* (this work), *Megerlia truncata* and *Terebratalia transversa* [*Griesshaber et al.*, 2007]. The highest hardness values in the secondary layers of the shells of the epibenthic brachiopods are present in the center of the compact layers. In the anterior parts of *Discradisca stella* the corrugated surface may lower the measured values systematically. Indents in the corrugated area have microhardness values of around 90 HV 0.05/10, whereas indents in the planar areas have around 120 HV 0.05/10. In the umbo region we find values up to 160 HV 0.05/10. *Discinisca laevis* has quite uniform hardness values of around 85 HV 0.05/10 that are lowered to ∼40 HV 0.05/10 in the center of the shell. This is caused by an intermediate organic stratum in the investigated individual. In other samples SEM analyses (not shown) revealed much less amount of this layer located only in the anterior and posterior part of the shell.

[19] We could identify crack-blunting and crack-bridging mechanisms (Figure 10) within all three shells. The investigated cracks were mainly caused by sample preparation and not by the Vickers indents, which cause cracks in calcitic brachiopod shells.

4. Discussion
4.1. Similarities and Differences Between the Studied Inarticulated Brachiopod Species

[20] The most common feature of the investigated phosphatic brachiopod shells is the compact layer. In the investigated species, this layer is formed when apatite crystallites grow onto strings of organic material, predominantly chitin fibers. The phosphate contributes hardness, stiffness, and wear resistance to the material, and the chitin provides flexibility. The nanoparticulate nature of the calcium phosphate allows the chitin fibers to predetermine the propagation direction of a potential crack. The twisted character of these fibers leads to the sawtooth-like shape of the cracks (Figure 10). Several apatite-chitin strings form thin lamellae, a dense array of lamellae builds compact
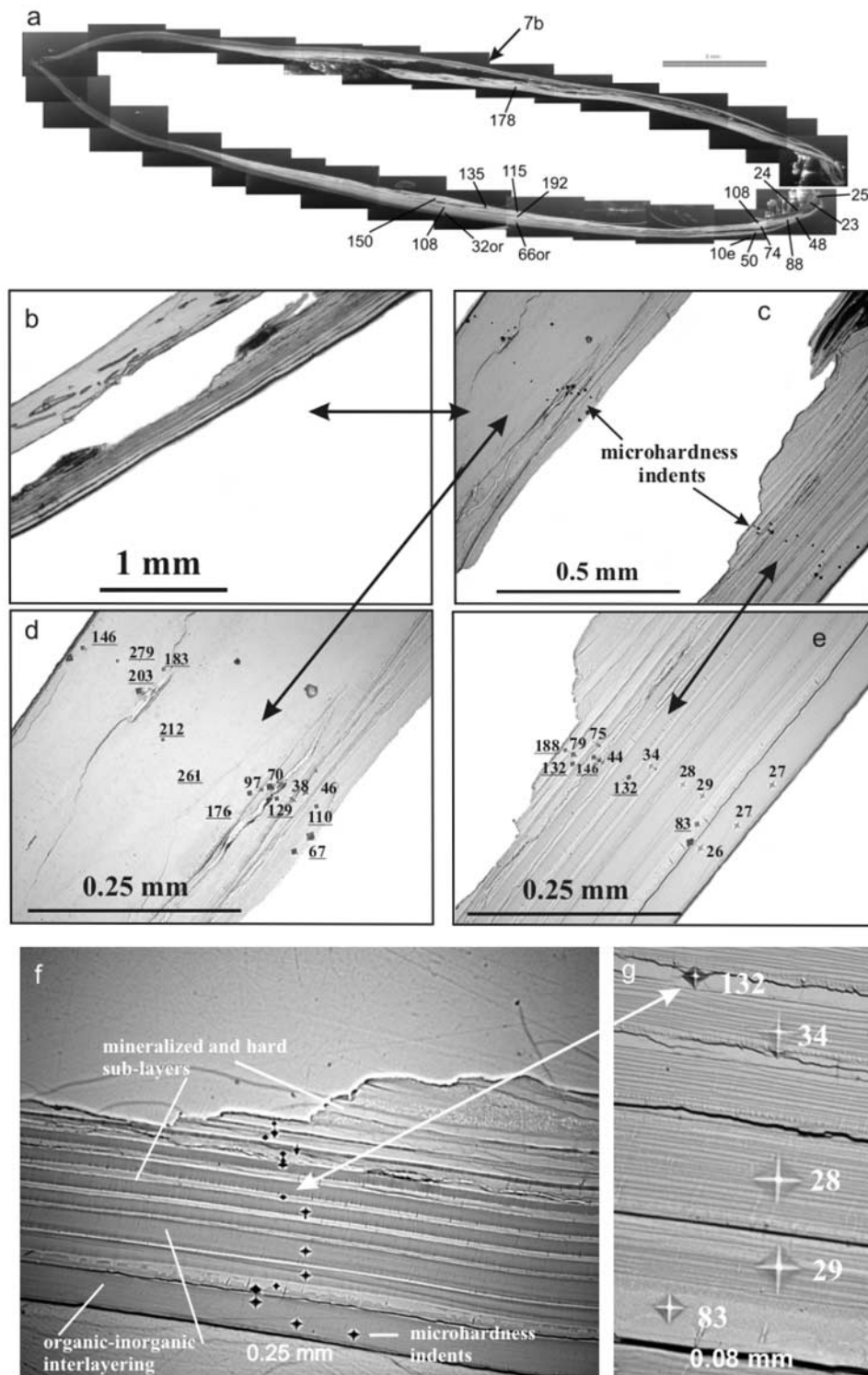
Figure 7. Microhardness distribution pattern in the shell of *Lingula anatina*. (a) Overall distribution pattern of microhardness. The indentations were performed with a force of 0.49 N. Scale bar is 5 mm. (b-e) Microindentation profile with small indents (force 0.049 N) in discrete shell laminae. (f, g) Detail of the microindentation profile shown in Figures 7b–7e. Underlined hardness values (Figures 7b–7e) are from indentations placed in the hard and mineralized laminae of the shell, while the other values represent indentations which were placed in the organic-dominated laminae. Not only the hardness values are significantly different (depending on whether they are indented in a predominantly mineralized or a predominantly organic-rich section) but also their shape. Clearly visible are the hardness differences between highly mineralized (hard) and the less-mineralized organic-rich shell layers. The organic-rich layers are best described as an interlayering of pure organic and inorganic-dominated lamellae.
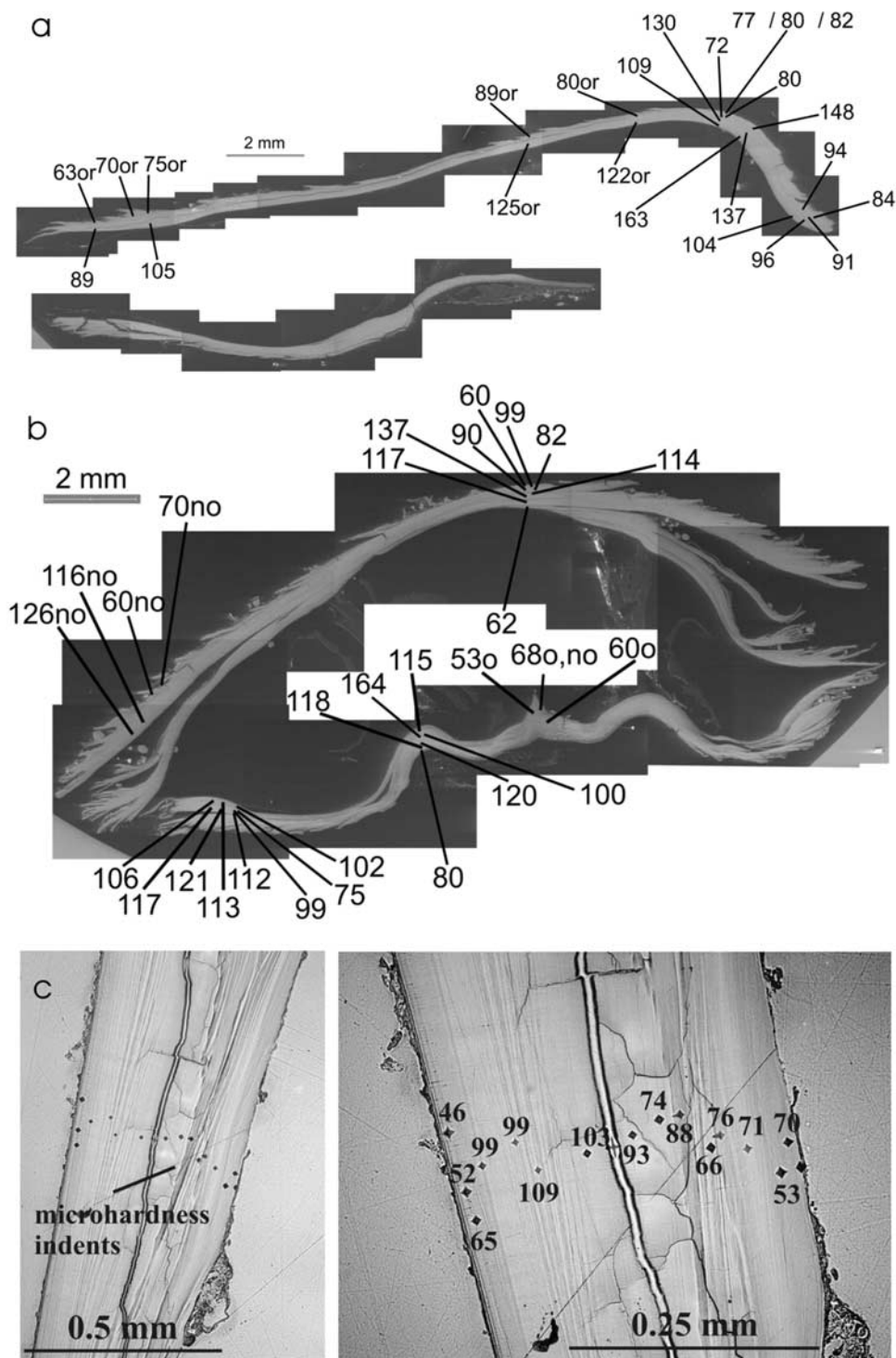
Figure 8. Microhardness distribution pattern in the shell of *Discradisca stella*. Figure 8a shows a longitudinal section whereas Figure 8b gives a cross cut through the shell. Circles indicate shell regions with baculate structures (see Figures 5 and 6). Scale bar is 2 mm. Microhardness indentations in Figures 8a and 8b were carried out with a force of 0.49 N, while the indentations shown in Figure 8c were done with a force of 0.049 N. The hardness distribution pattern is not straightforward, such that the shell is hard in its outermost layers and soft along its innermost segments.
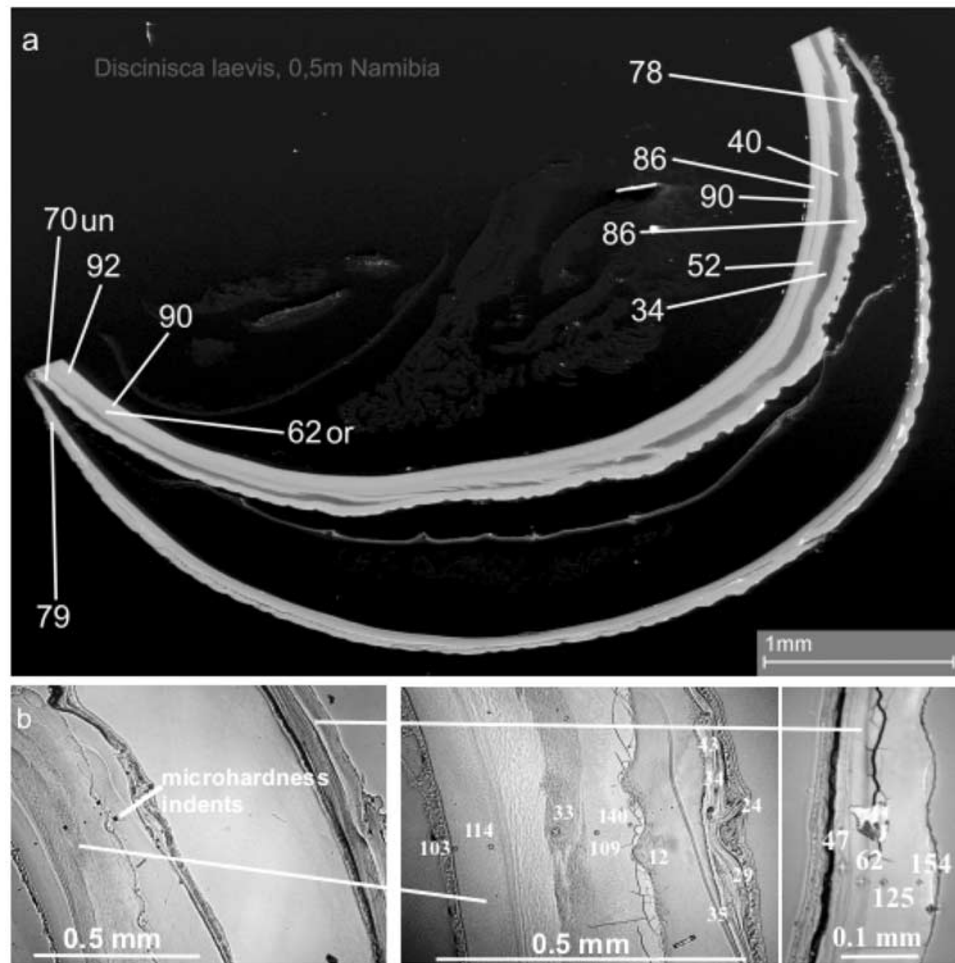
Figure 9. Microhardness distribution pattern in the shell of *Discinisca* laevis. The overall distribution pattern is shown in Figure 9a while a detailed distribution of hardness is presented in Figure 9b. The applied force was 0.49 N and 0.049 N for the indentations shown in Figure 9a and 9b, respectively.

layers with different thickness, and a succession of compact and pure organic layers forms the hybrid laminated composite material of the shell.

[21] Repeated occurrences of pure, extremely soft, organic layers with intercalations of thin hard mineralized compact layers provide flexibility and strength, especially in regions where high bending strains may occur (e.g., *Dicradisca stella*, Figure 8b). Transitional zones, where both, organic as well as inorganic phases are observable in the same layer are also present; however, they occur less often than pure organic and compact layers.

[22] According to specific habitat requirements in some forms the primary layer can even be entirely of organic material. This is the case for *Lingula anatina*, where the animal buries itself completely into the sediment and a flexible shell (Figure 7) is advantageous if the burrow narrows by sediment movements. In contrast to *Lingula anatina*, *Discradisca stella* and *Discinisca laevis* live above the sediment, and organic matter within their primary layer is much less important and serves as a matrix for the controlled formation of Ca-phosphate. The high hardness requirements (Figures 8 and 9) of the outer shell portion of these brachiopods are met through the incorporation of amorphous phosphate. A thin and hard primary layer

potentially serves as protective cover distributing forces across a larger area of the inner secondary shell layer. The secondary shell layer of all investigated species does not contain as much amorphous phosphate as the primary layer. While there is a laminate of organic and thin mineralized layers in *Lingula anatina*, there is just a small number (2−4) of sublayers of the secondary layer, and the mineralization is more uniform in the thick and sturdy compact layers of the shells of the two epibenthic brachiopod species. For *Discradisca stella* the apparently uniform layer is differentiated into two sublayers with different fracture behavior: a corrugated surface in the outer part of the shell and a planar surface in the inner part. The corrugation effect could be due to the pullout of fiber bundles, which are separated by either weak organic or brittle inorganic boundaries, which prescribe the corrugation.

[23] The uniqueness of a biomaterial, regardless whether it is calcite-, silica- or phosphate-dominated, is given by its hybrid composite nature and its complex hierarchical organization, where every structural level contributes to the function of the resulting material design [e.g., *Currey*, 2005; *Rousseau et al.*, 2005]. In the three phosphatic brachiopod species we could identify up to seven levels of structural hierarchy. In *Lingula anatina* for example the
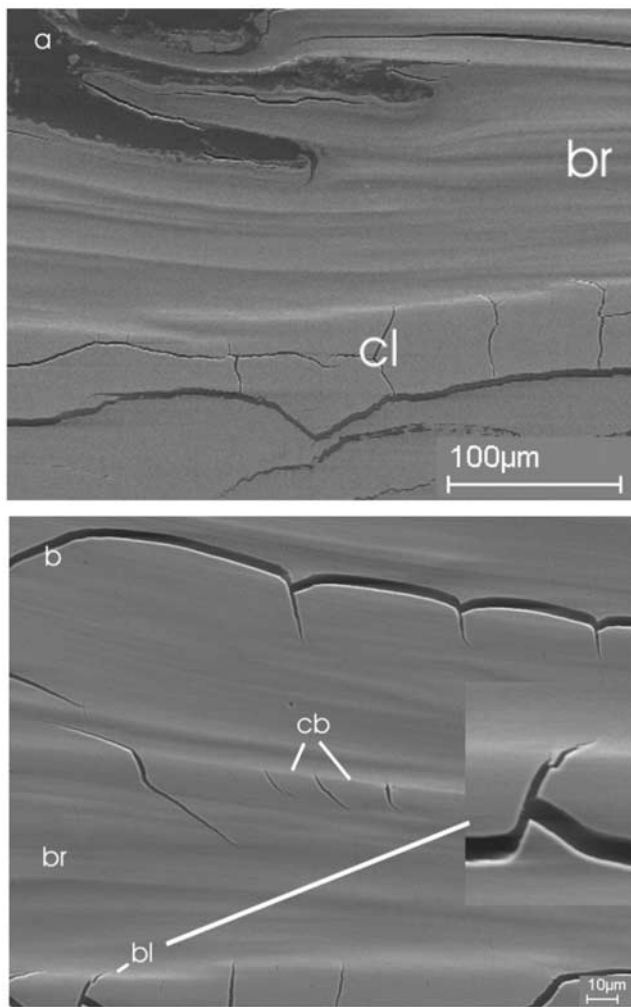
Figure 10. SEM images revealing behaviour of the secondary layer (compact layer) of *Discradisca stella*. (a) Fracture behaviour visible on the polished surface with a cleaving (cl) and a rough brittle (br) mode resulting in different morphologies (planar and corrugated) of the polished surface. (b) Crack-bridging (cb) and crack-blunting (bl) mechanisms in the brittle (strongly compact) section of the secondary layer.

first step is when organic fibers are formed, which in a second level are coated with nanometer-sized apatite particles. These organic-apatite strings are bundled together in the third structural level to thin lamellae, which in the fourth level form arrays and build the compact layer. The next higher structural level is characterized by lamination between pure organic portions and a compact layer. The rhythmic unit forms the fifth level of hierarchy, while repeated rhythmic units build the sixth level. The distinction between the primary and the secondary layer gives the last, seventh level of hierarchy.

[24] The most significant differences between the studied phosphatic brachiopod genera are given by the fraction of organics present either as pure organic layers and membranes or as organic matrix within the compact and baculate structures. The organic material is used in the investigated shells for two purposes: (1) As a template for the nucleation of mineral aggregate, and (2) as pure organic layers which lead to crack deviation and stop crack propagation.

4.2. Comparison to Modern Calcitic Brachiopod Shells

[25] A layered structure, comprising a primary, secondary (and occasionally tertiary) layer is also present in modern calcitic Terebratulide and Rhynchonellide articulated brachiopod shells [e.g., *Samtleben et al.*, 2001]. However, the well-defined organic layers and membranes of modern phosphatic brachiopods are absent in calcitic forms, even though intracrystalline and intercrystalline organics [*Curry et al.*, 1991; *Samtleben et al.*, 2001] also contribute decisively to the functional properties of calcitic shells as reflected, for example, in the hardness distribution pattern [*Griesshaber et al.*, 2007].

[26] While phosphatic brachiopods use amorphous phosphate to obtain an enhanced hardness and stiffness of their primary layer and phosphate crystals within the secondary layer for strengthening the shell structure, calcitic brachiopods build their primary layer from nano-sized, randomly shaped calcite crystallites [*Griesshaber et al.*, 2007] and compose their secondary layer from calcite fibers stacked in different directions [*Schmahl et al.*, 2004]. Therefore molecular structure (amorphous or crystalline), crystallite size and microstructural organization play an important role in providing functional materials properties (strength, hardness, stiffness) in both, phosphatic as well as calcitic brachiopod forms.

[27] In calcitic shells crack stopping and crack deviating mechanisms arise with the aid of organic sheaths that surround each calcite fiber. In phosphatic forms the colloidal structure of phosphate particles could have a crack deviating effect at the nanoscale. At the microscale the laminates of organic and inorganic layers impede crack propagation by crack-blunting and crack-bridging mechanisms within the strongly mineralized compact secondary layer of the shell (Figures 10a and 10b). These crack deviating mechanisms are highly energy-absorbing [e.g., *Kruzic et al.*, 2003] and, since crack propagation is predetermined parallel, rather than perpendicular to the surface of the shell, the migration of cracks through the entire shell is favorably controlled.

4.3. Comparison to Other Phosphatic Biomaterials

[28] Apart from the phosphatic shells of inarticulate brachiopods, vertebrate bone is the only other Ca-phosphatic biomaterial with a structural supporting function. These two materials (phosphatic brachiopod shells and bones) are similar indeed in many respects. Both are hybrid composites, with a particle or crystallite size of calcium phosphate in the range of tens of nanometers. Bone apatite crystals are usually found to be platelet-shaped with dimensions ranging on the order of $25-100$ nm length, $12-45$ nm width, and $2-6$ nm thickness [*Landis et al.*, 1996; *Erts et al.*, 1994; *Weiner and Price*, 1986; *Kim et al.*, 1995; *Ziv and Weiner*, 1994; *Fratzl et al.*, 1992; *Wachtel and Weiner*, 1994]. While the Ca-phosphate particles of the brachiopod shells (granules *in Williams and Cusack* [1999] terminology) are similar in size to bone apatite crystallites, they appear to be isometric rather than platelet shaped. A second analogy is the association of the calcium phosphate nanoparticles with organic fibers. For vertebrate bone, this is the protein collagen [*Kadler*, 1994; *Prockop and Fertala*,

1998], while for brachiopods it is mainly the carbohydrate chitin [*Iwata*, 1981; *Williams and Cusack*, 1999]. On higher length scales, the fracture-resistant structures of vertebrate bone can be somewhat more elaborate [*Currey*, 2002], however, than the laminate of the brachiopod shell structure. At present we have only the Vickers microhardness data as an estimate of mechanical stability. We observed that the microhardness is related to the content of inorganic phase, and we find values of $\sim$ 25 HV 0.05/10 for the pure chitin to $\sim$190 HV 0.05/10 for the strongly mineralized "compact" layers. The total organic content of the shell of *Lingula anatina* is about 40% [*Iwata*, 1981], whereas for *Discinisca laevis* and *Discradisca stella* it is about 25% [*Williams et al.*, 1994, 1998a]. For vertebrate bone or teeth the hardness also correlates with the amount of inorganic material in the mineralized structure, leading to a large range of hardness parameters between standard bony tissues, cement and dentine and highly mineralized bone and enamel [*Currey and Abeysekera*, 2003]. Human bony tissues have about 30% of organic content and the Vickers hardness is around 90 HV 0.05/10 [*Currey and Abeysekera*, 2003] and with a similar organic content tooth cement and dentine show 29 < HV 0.05/10 < 90.0. This order of magnitude compares well with the range of values found in the mineralized layers of the investigated brachiopod shells in this study (34 < HV 0.05/10 < 160). Human tooth enamel contains only about 1% of organic material that is mostly protein [*Waters*, 1980; *Currey*, 2002] and it reaches exceedingly high Vickers hardness between 270 and 375 HV 0.05/10 [*Currey and Abeysekera*, 2003].

5. Concluding Summary

[29] 1. The shells of modern, inarticulate brachiopods can be regarded as hybrid (i.e., organic/inorganic) composites. These particle reinforced fiber composites are used on the nanoscale by all investigated genera, which are used to construct hybrid laminated sequences on different length scales between predominantly inorganic and predominantly organic layers. The patterns of these laminates and the amount of incorporated phosphate in the shell is the most distinctive feature between the studied brachiopod genera. The primary layer of phosphatic brachiopods can be either entirely of organic material or it is composed of an organic matrix into which predominantly amorphous phosphate is embedded. In the secondary layer the animals incorporate crystalline calcium phosphate to a much higher content.

[30] 2. The hardness of the shell is given by the amount of incorporated phosphate, molecular structure of the used mineral, crystallite size and microstructural organization. These features are metabolically varied according to habitat requirements. The microhardness of inarticulate brachiopods compares well with the microhardness of bone and dentine. This can be attributed to the fundamental similarities in the fiber composite structure between the brachiopod shells and, for example, bone tissue at the microscale. The mechanisms to prevent crack propagation are comparable too. A remarkable feature of the brachiopod shell microstructure is the twisting of chitin fibers which leads to saw tooth shaped cracks along the relatively brittle compact layers.

[31] 3. We could identify up to seven levels of structural hierarchy in the shells. The specific use of varying fractions of organic and inorganic components together with a hierarchical design is an effective way to tune mechanical properties including the defense against crack formation and crack propagation. The hard outer layer (which is present in all epibenthic brachiopod forms) prevents most of the cracks forming and the lamination of the soft, organic-rich inner layer reduces stress concentration by distributing the force to a large area. If a crack nevertheless formed, the inner shell layer prevents crack propagation through crack-bridging and crack-blunting effects.

References

Aizenberg, J., J. C. Weaver, M. S. Thanawala, V. C. Sundar, D. E. Morse, and P. Fratzl (2005), Skeleton of Euplectella spp.: Structural hierarchy from the nanoscale to macroscale, *Science*, *309*, 275–278.

Brand, U., A. Logan, N. Hiller, and J. Richardson (2003), Geochemistry of modern brachiopods: Applications and implications for oceanography and paleoceanography, *Chem. Geol.*, *198*, 305–334.

Bruckschen, P., S. Oesmann, and J. Veizer (1999), Isotope stratigraphy of the European carboniferous: Proxy signals for ocean chemistry, climate and tectonics, *Chem. Geol.*, *161*, 127–163.

Cölfen, H., and S. Mann (2003), Higher-order organization by mesoscale self-assembly and transformation of hybrid nanostructures, *Angew. Chem. Int. Ed.*, *42*, 2350–2365.

Currey, J. (Ed.) (2002), *Bones: Structure and Mechanics*, 436 pp., Princeton Univ. Press, Princeton, N. J.

Currey, J. (2005), Hierarchies in biomineral structures, *Science*, *309*, 253–254.

Currey, J., and R. M. Abeysekera (2003), The microhardness and fracture surface of the petrodentine of Lepidosiren (Dipnoi), and of other mineralised tissues, *Arch. Oral Biol.*, *48*, 439–447.

Curry, G., M. Cusack, D. Walton, K. Endo, H. Clegg, G. Abbott, and H. Armstrong (1991), Biogeochemistry of brachiopod intracrystalline molecules, *Philos. Trans. R. Soc., Ser. B*, *333*, 359–366.

Erts, D., L. J. Gathercole, and E. D. T. Atkins (1994), Scanning probe microscopy of intrafibrillar crystallites in calcified collagen, *J. Mater. Sci. Mater. Med.*, *5*, 200–206.

Fratzl, P., M. Groschner, G. Vogt, H. Plenck, J. Eschberger, N. Fratzl-Zelman, K. Koller, and K. Kalushofer (1992), Mineral crystals in calcified tissues: A comparative study by SAXS, *J. Bone Miner. Res.*, *7*, 329–334.

Gilbert, P. U., M. Albrecht, and B. H. Frazer (2005), The organic-mineral interface in biominerals, *Rev. Miner. Geochem.*, *59*, 157–185.

Griesshaber, E., W. Schmahl, R. Neuser, R. Job, M. Bluem, and U. Brand (2005), Microstructure of brachiopod shells—An inorganic/organic fiber composite with nanocrystalline protective layer, *Mater. Res. Soc. Symp. Proc.*, *851*, 99–104.

Griesshaber, E., W. Schmahl, R. Neuser, T. Pettke, M. Blüm, and U. Brand (2007), Texture and microstructure of terebratulide brachiopod shell calcite—An optimized materials design with hierarchical architecture, *Am. Miner.*

Iijima, M., and Y. Moriwaki (1990), Orientation of apatite and organic matrix in Lingula unguis shell, *Calcif. Tissue Int.*, *47*, 237–242.

Iwata, K. (1981), Ultrastructure and mineralization of the shell of Lingula unguis Linne (inarticulate brachiopod), *J. Fac. Sci. Hokkaido Univ. Ser. IV*, *20*(1), 957–966.

Ji, B., and H. Gao (2004), A study of fracture mechanisms in biological nano-composites via the virtual internal bond model, *Mater. Sci. Eng. A*, *366*, 96–103.

Kadler, K., (Ed.) (1994), Extracellular matrix, 1: Fibril-forming proteins, in *Protein Profile*, edited by P. Sheterline, pp. 517–638, Elsevier, New York.

Kamat, S., X. Su, R. Ballarini, and A. H. Heuer (2000), Structural basis for the fracture toughness of the shell of the conch Strombus gigas, *Nature*, *405*, 1036–1040.

Kim, H. M., C. Rey, and M. J. Glimcher (1995), Isolation of calcium-phosphate crystals of bone by nonaqueous methods at low temperature, *J. Bone Miner. Res.*, *10*, 1589–1601.

Kruzic, J., R. Nalla, J. Kinney, and R. Ritchie (2003), Crack blunting, crack bridging and resistance-curve fracture mechanics in dentin: Effect of hydration, *Biomaterials*, *24*, 5209–5221.

Landis, W. J., K. J. Hodgens, J. Arena, M. J. Song, and B. F. McEwen (1996), Structural relations between collagen and mineral in bone as determined by high voltage electron microscopic tomography, *Microsc. Res. Tech.*, *33*, 192–202.

Laraia, V., and A. Heuer (1990), The nanoindentation behaviour of several mollusk shells, *Mater. Res. Soc. Symp. Proc.*, *174*, 125–131.

Lévêque, I., M. Cusack, S. A. Davis, and S. Mann (2004), Promotion of fluoroapatite crystallization by soluble-matrix proteins from Lingula Anatina shells, *Angew. Chem. Int. Ed.*, *43*, 885.

Mayer, G. (2005), Rigid biological systems as models for synthetic composites, *Science*, *310*, 44–47.

Mayer, G., and M. Sarikaya (2002), Rigid biological composite materials: Structural examples for biomimetic design, *Exp. Mech.*, *42*(4), 395–403.

Okumura, K., and P. G. De Gennes (2001), Why is nacre strong? Elastic theory and fracture mechanics for biocomposites with stratified structures, *Eur. Phys. J. E*, *4*(1), 121–127.

Oyen, M. L., A. J. Bushby, A. Mann, and C. Ortiz (Ed.) (2006), Mechanics of biological and biomimetic materials at small length-scales, *J. Mater. Res.*, *21*, 287 pp.

Parkinson, D., G. B. Curry, M. Cusack, and A. E. Fallik (2005), Shell structure, patterns and trends of oxygen and carbon stable isotopes in modern brachiopod shells, *Chem. Geol.*, *219*, 193–235.

Prockop, D. J., and A. Fertala (1998), The collagen fibril: The almost crystalline structure, *J. Struct. Biol.*, *122*, 111–118.

Rousseau, M., E. Lopez, P. Stempfle, M. Brendle, L. Franke, A. Guette, R. Naslain, and X. Bourrat (2005), Multiscale structure of sheet nacre, *Biomaterials*, *26*, 6254–6262.

Samtleben, C., A. Munnecke, T. Bickert, and J. Pätzold (2001), Shell succession, assemblage and species dependent effects on C/O-isotopic composition of brachiopods—Examples from Silurian of Gotland, *Chem. Geol.*, *175*, 61–107.

Sarikaya, M., H. Fong, N. Sunderland, B. D. Flinn, G. Mayer, A. Mescher, and E. Gaino (2001), Biomimetic model of a sponge-spicular optical fibre—Mechanical properties and structure, *J. Mater. Res.*, *16*, 1420–1437.

Sarikaya, M., C. Tamerler, D. T. Schwartz, and F. O. Baneyx (2004), Materials assembly and formation using engineered polypeptides, *Annu. Rev. Mater. Res.*, *34*, 373–408.

Schmahl, W. W., E. Griesshaber, R. Neuser, A. Lenze, and U. Brand (2004), Morphology and texture of the fibrous calcite in terebratulide brachiopode shells, *Geochim. Cosmochim. Acta*, *68*(11), Suppl. SA202.

Sundar, V. C., A. D. Yablon, J. L. Grazul, M. Ilan, and J. Aizenberg (2003), Fibre-optical features of a glass sponge—Some superior technological secrets have come to light from a deep-sea organism, *Nature*, *434*, 890–899.

Veizer, J., et al. (1999), Sr-87/Sr-86, delta C-13 and delta O-18 evolution of Phanerozoic seawater, *Chem. Geol.*, *161*(1-3), 59–88.

Wachtel, E., and S. Weiner (1994), Small-angle X-ray scattering study of dispersed crystals from bone and its mechanical stiffness, *J. Bone Miner. Res.*, *9*, 1651–1655.

Waters, N. E. (1980), Some mechanical and physical properties of teeth, in *The Mechanical Properties of Biological Materials*, *Symp. Soc. Exper. Biol.*, vol. 34, edited by J. F. V. Vincent and J. D. Currey, pp. 99–135, Cambridge Univ. Press, New York.

Wegst, U. G. K., and M. F. Ashby (2004), The mechanical efficiency of natural materials, *Philos. Mag.*, *84*(21), 2167–2181.

Weiner, S., and P. A. Price (1986), Disaggregation of bone into crystals, *Calcif. Tissue Res.*, *39*, 365–375.

Williams, A., and M. Cusack (1999), Evolution of a rhythmic lamination in the organophosphatic shells of brachiopods, *J. Struct. Biol.*, *126*, 227–240.

Williams, A., M. Cusack, and S. Mackay (1994), Collagenous chitino-phosphatic shell of the brachiopod Lingula, *Philos. Trans. R. Soc., Ser. B*, *346*, 223–266.

Williams, A., et al. (1997), Brachiopoda, in *Treatise on Invertebrate Paleontology, Part H*, pp. 265–526, Geol. Soc. of Am., Boulder, Colo.

Williams, A., M. Cusack, J. Buckman, and T. Stachel (1998a), Siliceous tablets in the larval shells of apatitic discinid brachiopods, *Science*, *279*, 2094–2096.

Williams, A., M. Cusack, and J. Buckmann (1998b), Chemico-structural phylogeny of the discinoid brachiopod shell, *Philos. Trans. R. Soc., Ser. B*, *353*, 2005–2038.

Ziv, V., and S. Weiner (1994), Bone crystal sizes: A comparison of transmission electron microscopic and X-ray diffraction line width broadening techniques, *Connect. Tissue Res.*, *30*, 165–175.

————————

E. Griesshaber, Section of Palaeontology, Department of Earth and Environmental Sciences, Ludwig-Maximilians University Munich, Luisenstrasse 37, D-80333 Munich, Germany. (e.griesshaber@lrz-uni.muenchen.de)

G. Jordan, C. Merkel, and W. W. Schmahl, Section of Applied Crystallography and Materials Science, Department of Earth and Environmental Sciences, Ludwig-Maximilians University Munich, Theresienstrasse 41, D-80333 Munich, Germany. (guntram.jordan@lrz.uni-muenchen.de; casjen.merkel@lrz.uni-muenchen.de; wolfgang.schmahl@lrz.uni-muenchen.de)

K. Kelm and W. Mader, Institut für Anorganische Chemie, Universität Bonn, Römerstrasse 164, D-53117 Bonn, Germany. (kelm@uni-bonn.de; madder@uni-bonn.de)

A. Logan, Department of Physical Sciences, University of New Brunswick, P.O. Box 5050, Saint John, New Brunswick, Canada E2L 4L5. (logan@unbsj.ca)

R. Neuser, Institut für Geologie, Mineralogie und Geophysik, Ruhr-Universität Bochum, Universitätsstrasse 150, D-44780 Bochum, Germany. (rolf.neuser@ruhr-uni-bochum.de)